



Hardware Article

A versatile hot melt centrifugal spinning apparatus for thermoplastic microfibres production

Jason Gunther, Jacques Lengaigne, Mélanie Girard, Valérie Toupin-Guay, James T. Teasdale, Martine Dubé, Ilyass Tabiai*

CREPEC, Department of Mechanical Engineering, École de technologie supérieure, 1100 Notre-Dame Street West Montreal, QCH3C 1K3, Canada



ARTICLE INFO

Keywords:

Centrifugal spinning
Melt
Microfibre
Nonwoven textile
Nozzlefree
Processing

ABSTRACT

The centrifugal spinning (CS) method could address common issues such as low production rate and high energy consumption in the industry of nonwoven textile fabrication. Similarly to cotton candy production, the high-speed rotating reservoir extrudes melt or solvent-based polymer from orifices to produce fibres. Using polymer melt avoids solvent elimination and toxicity, but the process is more difficult. Thus, a versatile lab-scale hot melt spinneret with the ability to pour pellets inside continuously to expand our knowledge of the CS method and investigating different extrusion geometries such as nozzlefree is developed. Among the controllable parameters are, the spinneret heating temperature (up to 300°C), its two interchangeable 3D printer nozzles. An Arduino code is used to stabilize the temperature. The system performance is investigated with polypropylene and polylactide. The results show that fibres under 15 µm in diameter are produced. This work is licensed under CC BY-NC 4.0. To view a copy of this license, visit <http://creativecommons.org/licenses/by-nc/4.0/>.

1. Specifications table

Hardware name	Hot melt centrifugal spinning apparatus
Subject area	<ul style="list-style-type: none"> • Engineering and material science • Nonwoven textile • Polymer fibre production • Open source alternatives to existing infrastructure
Hardware type	<ul style="list-style-type: none"> • Tissue engineering • Woven engineering
Closest commercial analog	The hardware uses components from the GoldMedalSuperflossMaxx™ cotton candy machine [1]. The closest commercial analogs are the Fiberio FX2200 [2], the Nanocentrino L1.0 from Areka [3] and the Cyclone Pilote G1 from Pardam Nano4Fibers [4,5]. These commercial machines mostly produce fibres with solvent-based polymer solutions while the hardware presented here uses hot melt polymers.
Open source license	This work is licensed under CC BY-NC 4.0. To view a copy of this license, visit http://creativecommons.org/licenses/by-nc/4.0/

(continued on next page)

* Corresponding author.

E-mail address: ilyass.tabiai@etsmtl.ca (I. Tabiai).

<https://doi.org/10.1016/j.ohx.2023.e00454>

Available online 15 July 2023

2468-0672/© 2023 The Author(s). Published by Elsevier Ltd. This is an open access article under the CC BY-NC-ND license (<http://creativecommons.org/licenses/by-nc-nd/4.0/>).

(continued)

Hardware name	Hot melt centrifugal spinning apparatus
Cost of hardware	2 662.16 \$ (2021–2022)
Source file repository	On Open Science Framework (OSF) with DOI: 10.17605/OSF.IO/JH6QY[6]

2. Hardware in context

Centrifugal spinning (CS) (also called rotary jet spinning or RJS) allows for the production of micrometric and submicrometric fibres for applications such as nonwoven textiles and filtration membranes. CS offers a high production rate compared to electrospinning which is currently the laboratory workhorse in the field. Reported production rate for a commercial electrospinning machine was 210 g/h [2]. This is much lower than the 12 000 g/h [2] production rate reported for a commercial CS machine. In addition, its low energy consumption and simple design makes it interesting for industrial production compared to meltblown [2,7]. Meltblown is the most common process in the nonwoven textile industry because of its high production rate (up to 1500 g/h) [2]. In meltblown, polymer pellets are melted by an extruder before being extruded from a die by a heated airflow. Fibre formation begins at the exit of the die. The high airflow needs to be heated at a temperature much higher than the melting point of the polymer feedstock to extrude the melt. In a previous work from Wongpajan and al. [8], polypropylene (PP) fibres were produced through an apparatus that works similarly to meltblown. While their PP feedstock melted between 280–350°C, the airflow used to extrude the melt was maintained at 600°C [8] constantly. CS fibre production is achieved either from solvent-based polymer solution or from pure polymer melt. However, most published works on CS deal with polymer solutions rather than melt [2,7]. Indeed, the main challenge for the latter is to maintain a high temperature at the high rotation speed needed for hot melt flow. To the authors knowledge, no detailed hot melt CS apparatus description is available in the literature, limiting the development of the process. This article presents such a setup based on a common architecture inspired by a commercially available cotton candy machine. It aims at providing a simple and versatile apparatus for anyone looking to produce microfibrils directly from polymer melt. The setup overview is presented in Fig. 1 and is further described in the following section.

Description of the CS process

Hot melt CS works similarly to a cotton candy machine. Polymer pellets, instead of sugar, are fed in a rotating reservoir called the spinneret. The spinneret is composed of an emitter, orifices and heating elements. The emitter is a cylindrical container where pellets are dropped. The orifices, which may usually be nozzles or grids, are found along the emitter wall. The heating elements inside the emitter can be cartridges, tubular elements, bands, or others. When the polymer melts, it is ejected by the centrifugal force (F_ω) through the orifices leading to fibre formation (the same way sugar filaments are produced in a cotton candy machine). The centrifugal force comes from the motor's rotational speed (ω in Fig. 1 and 2) and the spinneret radius. The different fibre production steps are presented in Fig. 2. Due to the viscous force, generated from the polymer melt viscosity, opposing the centrifugal force outside of the emitter, the ejected polymer filament, called the jet, is elongated (Fig. 2a) and solidified (Fig. 2b) until it reaches a collecting device, the collector. The fibre production stops when no pellets remain in the spinneret (Fig. 2c).

Similar work in the commerce and the literature

There are few existing commercial hardware, presented in Table 1 and they are designed to work with solvent-based polymer only. To the best of our knowledge, no equivalent machines are currently commercially available for polymer melt.

Different approaches are suggested in the literature to adapt the CS technique to the laboratory scale. Rajendran and al. [10] designed a low cost industrial centrifugal machine that could maintain the same fibre quality as the high-cost machines. The hardware

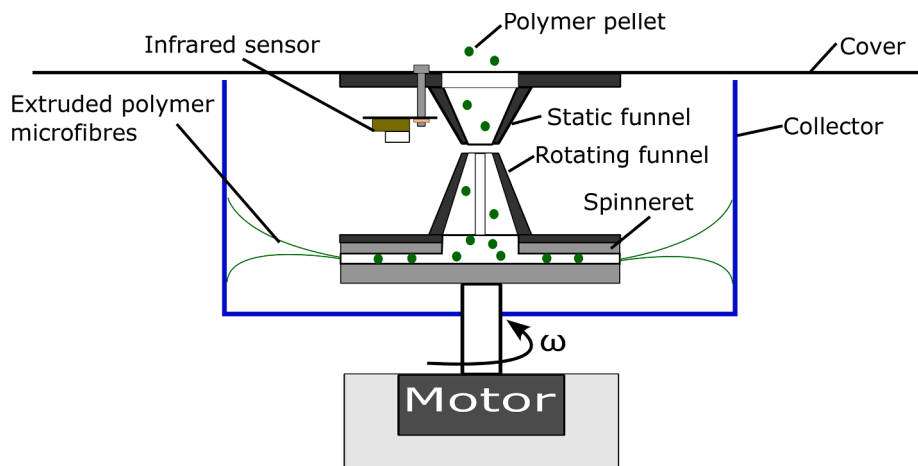


Fig. 1. Hot melt centrifugal spinning apparatus. Polymer pellets are introduced inside the rotating funnel and begin to melt. Once the pellets have fully melted, the centrifugal force created by the motor's rotational speed extrudes the polymer melt from the two channels inside the spinneret and jet formation begins. The fibres are gathered around the collector.

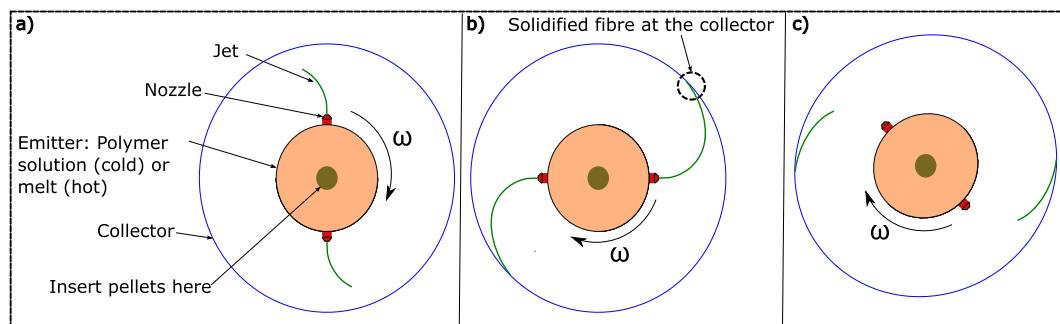


Fig. 2. Fibre production cycle by centrifugal spinning. The jet is elongated and cooled (a) until fully cooled when it reaches the collector (b). Fibre production continues until the spinneret is empty (c).

is interesting to study the commercial production of polymer solution fibres whereas it is not adapted for molten polymers. To produce fibres from polymer melts, Suttiruengwong et al. [11] modified a cotton candy machine to be able to control temperature and rotation speed. They studied the influence of both parameters on the fibre production. However, while they claim to prevent thermal degradation with this technique, they obtained polymer chains with a much lower molecular weight than the original material.

With their own design, Sebe and al. [12] studied the influence of the spinneret geometry such as its size, material quality, method of fixation to the motor and level of customization on fibre production. A spinneret with an appropriate size securely mounted to the motor increases its stability which allows it to rotate at higher speed. On the other hand, adequate material selection for the hardware is important to withstand the creep that can be caused by the centrifugal force. For this purpose, materials with high mechanical strength such as highly machinable Al7076 aluminum, polyethylene terephthalate (PET) and CuSn12 phosphor bronze were chosen by Sebe et al. [12] to build the reservoir and AISI304 stainless steel for the nozzles of their devices. Finally, they were able to change the nozzle size without disassembling the spinneret allowing for an interesting customization. It must be noted that the spinneret in this article is applied to solvent-based polymer solutions, but the conclusions about the hardware could be adapted to melts too, replacing PET used to build the hardware with a more heat-resistant material.

Other techniques may be used to produce fibres. Dominguez et al. [13] made a low-cost device based on solution blow spinning. In this technique, the polymer is dissolved in a solvent and injected into the machine using a pressurized gas. Mitropoulos et al. [14] developed a tunable wet spinning process to offer an alternative for researchers from existing expensive industrial techniques. Alternatively, Huang et al. [15] worked on an electrospinning/electrospraying fabrication technique using fused deposition modeling. While no fabrication experiment is presented in their paper, it also provides a much cheaper solution compared to existing commercial hardware.

3. Hardware description

Our system, illustrated in Fig. 1 consists of four modules: (1) a mechanical framework based on a commercial cotton candy machine, (2) a rotating head, (3) sensors and control electronic and (4) the collector-enclosure. Each module is described from Section 3.1–3.4.

3.1. Mechanical framework

This prototype is based on the commercial *GoldMedalSuperflossMaxxTM* cotton candy machine (see Fig. 3). The AC motor and its support frame are used without any modification. The motor directly drives rotation at a fixed speed of 3450 rpm (60 Hz AC). The frame is composed of a suspension system with four stiff springs allowing it to dampen the vibrations induced during operation. The slip ring assembly generates electrical power by friction with fixed carbon brushes during rotation. This power is then transmitted to the heaters.

3.2. The rotating head

The original rotating head illustrated in Fig. 3 is replaced with a custom head designed to produce polymer melt fibres (see Fig. 4).

Table 1

Existing commercial hardware.

Hardware name	Company	Production Rate	Number of Nozzles	Polymer state	References
FX2200	FibeRio	12 000 g/h	2	Mostly solvent-based (possible with melt)	[2]
Nanocentrino L1.0	Areka Group	50 ml/h/rotor	2	Solvent-based	[9]
Cyclone Pilot G1	Pardam Nano4Fibers	over 100 g/day	16	Solvent-based	[5]



Fig. 3. GoldMedalSuperflossMaxx™ cotton candy machine with the original spinneret.

This head is composed of an aluminum spinneret, a head support, two heaters, two nozzles and a funnel for continuous feeding. The spinneret is the most important component of the CS process because its design influences the fibre quality. Inside the spinneret, polymer pellets circulate through a straight horizontal channel up to the nozzles at both ends. They are ejected in fibres once they get hot enough. We use conventional 3D printing machine nozzles, which are easily replaceable if another size is needed. Instead of using these nozzles, it could also be possible to use a nozzlefree extrusion system with an adjustable slit or an inverted-T configuration. These three possibilities are illustrated in Fig. 4. Then, two horizontal heating cartridges inside the spinneret melt the pellets. The funnel is attached at the top of the spinneret. While its use is a tremendous advantage because the spinneret can be fed with pellets continuously, fibre production is possible without it. Finally, the head support connects the spinneret to the machine motor. It could be adjusted and machined to fit any other motor (from another commercial cotton candy machine or even from a custom setup).

3.3. Instrumentation and control electronics

Fig. 5 presents the circuit diagram of the apparatus. The original control unit was replaced and the electrical circuit was laid out externally to implement a fully controllable and safety-oriented circuit. The circuit is composed of two independent sub-arrangements: one for the heaters and one for the motor. Each consists of an on-off switch, a 20 A safety breaker, and a normally open relay. The relays are directly connected to an emergency stop button, to immediately open both circuits. In the sub-arrangement of the heaters,

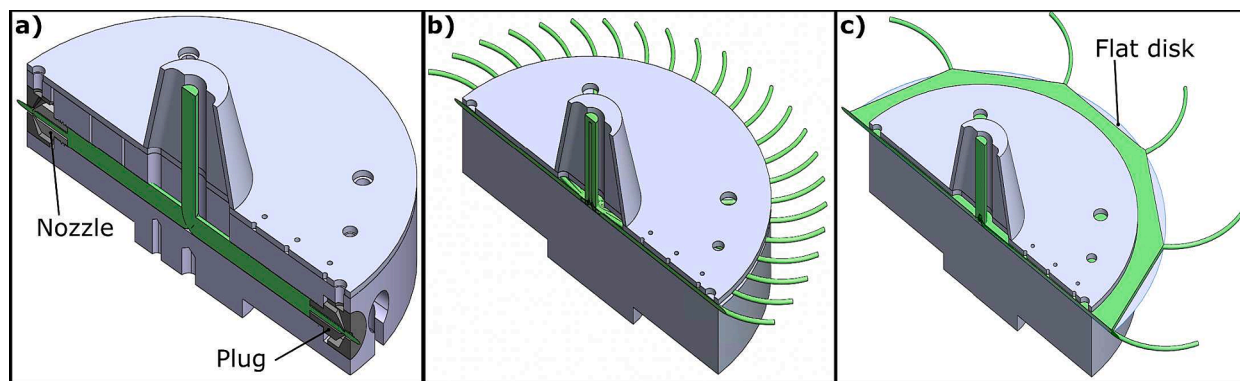


Fig. 4. Extrusion configurations with continuous feeding. Nozzles (a), nozzlefree with adjustable slit (b) and inverted-T (c) extrusion configurations. The inverted-T configuration is similar to (b), but the circular flat disk where the melt is extruded is larger than the spinneret.

the transmitted power is controlled by a 0–120 V manual rheostat while a proportional–integral–derivative (PID) code from an Arduino UNO stabilizes the temperature. The Arduino code compares the temperature between the value set by the user with a manual potentiometer and the measurement read from an infrared sensor (IR). Once the sensor reads the temperature selected by the user, the Arduino code opens up the circuit, thus deactivating the heaters in the spinneret. If the temperature read by the IR sensor is below the set temperature, the Arduino code closes the circuit to heat up the spinneret. The data generated by the Arduino code is viewed through Serial Studio, an open-source data viewer available on Github [16].

The IR sensor in Fig. 1 reads the temperature of the spinneret metal surface and it was calibrated with the default parameters. The assembling instructions of the IR sensor are discussed in Section 6.3.

The viewer displays the following data:

- Mission status: Displays the code run-time in seconds.
- PID set point: Displays the temperature set by the user that the spinneret has to reach in °C.
- Temp ON–OFF: Displays whether the heaters are heating (100%) or not (0%).
- IR ambient: Displays the environment ambient temperature in °C.
- IR reading: Displays the temperature read from the IR sensor in °C.
- Heater AC current: Displays the heater current in Amperes.

3.4. Enclosure and collector

The aluminum bowl from the original cotton candy machine is used for fibre collection. However, it could be replaced by collector with a different geometry to control its distance with the spinneret, as it influences the fibre morphology [17]. One possibility for instance would be to install vertical poles around a flat disk. This geometry is used in the FX2200 [2]. Most papers studied the influence of collector distance [18,19,17] rather than its geometry so it is unclear how this parameter influences fibre morphology. In addition here, an impact-resistant acrylic cover is placed on the collector to protect the user from any pellets or fibres flying off from the spinneret. It also helps maintain a constant temperature around the spinneret by preventing continuous heat loss due to the process's high rotation speed.

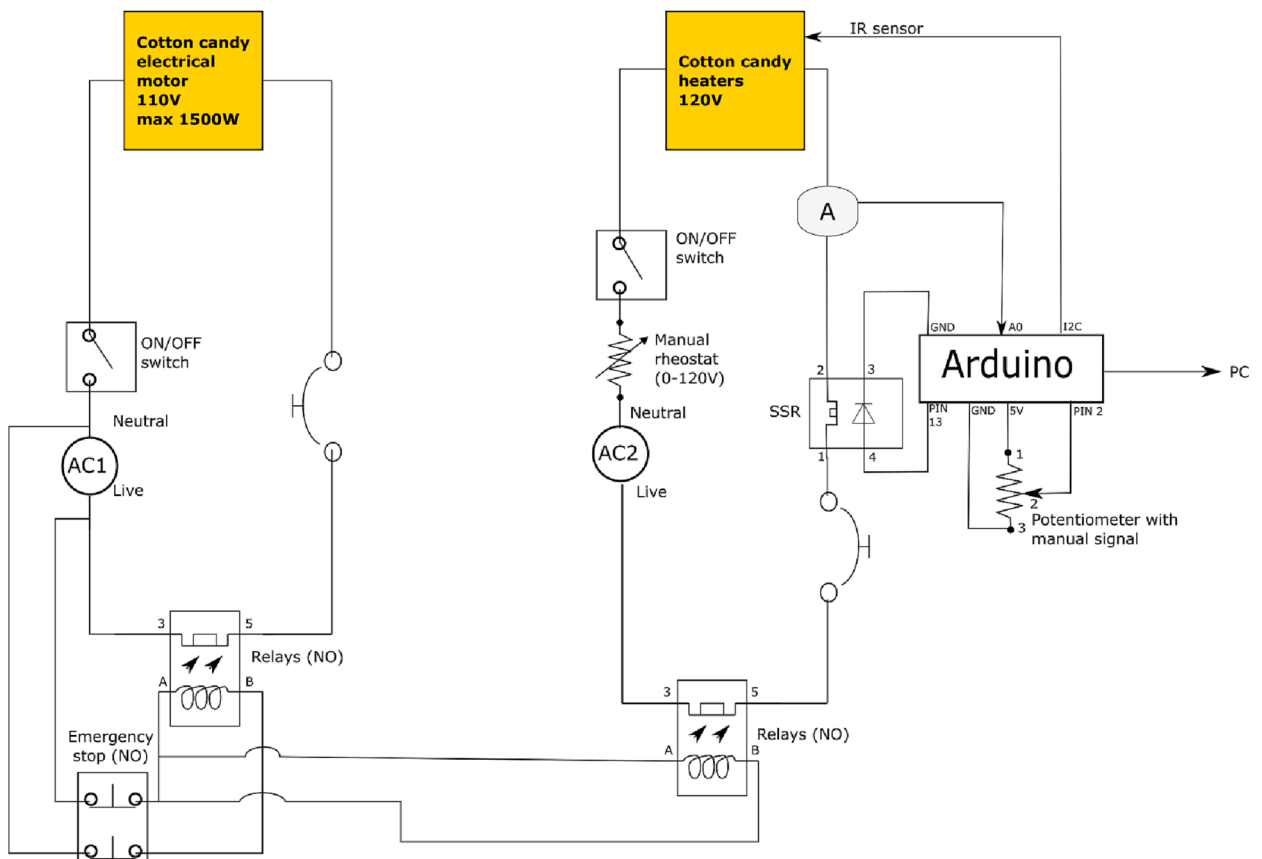


Fig. 5. Electronic layout of the apparatus.

3.5. Advantages of the design

Most articles use commercial CS machines (Tab. 1) to produce solvent-based polymer fibres [5,9,4]. While the main parameters to produce fibres with a custom designed hot melt CS apparatus, such as the spinneret, orifice and collector radius, the rotational speed and the heating temperature are shared in published studies, the overall design and components of the apparatus, such as the spinneret drawings and the selection of the motor and the heating elements (cartridges, bands, induction coils, etc.), are not. Thus, repeatability is challenging when a study uses an experimental hot melt CS apparatus. As explained in Section 2, heating the spinneret at high-rotational speed is challenging. Herein, a design with two powerful heating cartridges inside the spinneret to overcome this issue is suggested. Additionally, the feeding rate is an important aspect of our setup. Here, a fixed funnel for continuous feeding allows fibre formation for a prolonged period possible. Another strength of our design is its versatility presented in Fig. 4. From the extrusion geometry to the collector, different configurations can be experimented with. As an example, nozzlefree extrusion is done by simply elevating the funnel with washers or a metallic grid while closing the pellets entrance on the emitter with heat resistant tape to extrude melt on its surface. Moreover, the nozzles are standard parts that are easily exchangeable to work with different sizes. PID allows controlling the spinneret temperature at a desired value while sensors can be used to read the temperature automatically. Finally, while the main objective of this device is to produce polymer fibres from polymer melt, it could readily be used with solvent-based polymers by not heating the spinneret.

4. Design files

Table 2 lists the files of the custom parts of the machine. Components were either designed in CATIA or Solidworks and their files were converted to the STEP format to switch between softwares. 3D printed parts were converted into STL files and the G-codes were prepared in Cura. The codes for PID and temperature visualization are also presented in Table 2. All files are located in the Open Science Framework (OSF) project in [6] under the CC BY-NC 4.0 licence <http://creativecommons.org/licenses/by-nc/4.0/>.

- Spinneret head: Part that produces fibres (see Item 1). Polymer melt flows through the two channels.
- Head support: Part connected to the motor and supporting the spinneret head (see Item 2).
- Nozzle plug: Part preventing fibre dislocation when polymer melt is ejected from the nozzle (see Fig. 4a or Item 3). Using the plugs is optional as the resulting fibres remain satisfactory without them. The plugs also expand at high temperatures; thus removing them can be hard.
- Rotating funnel: Part used to feed the spinneret with polymer pellets continuously. The rotating funnel is made of two parts: the Draft and the Disk. These parts are welded together.
- Lower spinner head: This part is included with the *GoldMedalSuperflossMaxxTM* machine (see Item 22), but it needs to be modified in order to fix the head support to the rest of the machine.
- Static Funnel and Support: 3D printed parts used to feed the spinneret with pellets. The file contains two parts: the static funnel (see Item 40) and the static funnel support (see Item 41). The static funnel is also used to hold the temperature sensor.
- Collector: Part of the *GoldMedalSuperflossMaxxTM* machine used to collect the fibres.
- PID_SciRJS_sensor_acquisition: Code used to control the spinneret temperature.
- Serial_studio_formatting_Rev2: Code used to display through Serial Studio the data generated from PID_SciRJS_sensor_acquisition.

The remaining files to assemble the spinneret are in the online repository [6] has supplementary material.

5. Bill of materials summary

The bill of materials (BOM) is presented in Table 3 and Table 4. Table 3 details both standard and custom parts used to build the machine and Table 4 specifies printed parts of the apparatus. The BOM for the electrical components is presented as supplementary material in the open-access online file. All prices in the BOM are in Canadian dollars and dated from 2021–2022. In Table 4, the price of a whole filament was used instead of calculating the individual price for each component. For the custom parts, prices of the raw materials needed to build them are reported. The lower spinner head (Item 22) from the *GoldMedalSuperflossMaxxTM* machine is the

Table 2
Design files summary.

Design file name	File type
Spinneret head	Catia and STEP
Head support	Catia
Nozzle plug	Catia
Rotating funnel	Solidworks
Lower spinner head	Solidworks
Static Funnel and Support	Solidworks and STL
Collector	Solidworks
PID_SciRJS_sensor_acquisition	Arduino
Serial_studio_formatting	JavaScript Object Notation (JSON)

Table 3

Bill of materials for both standard and custom parts of the apparatus.

No. ARTICLE	Designator	Component	QTY	Cost per unit - currency	Total cost - currency	Supplier	Material type
1	Device build	Spinneret head	1	30.20 \$	30.20 \$	-	Metal
2	Device build	Head support	1	17.44 \$	17.44 \$	-	Metal
3	Device build	Nozzle plug	2	0.27 \$	0.54 \$	-	Metal
4	Device build	Funnel	1	37.85 \$	37.85 \$	-	Metal
5	Heating cartridge, 0.375" (9.258 mm) dia × 3" (76.2 mm) long, 120 V 500 W, 10" (254 mm) fiberglass wires,	CT-.38 × 3.00-120 - 500	2	254.26 \$	508.52 \$	Volton	Electronics
6	Circular ring connector 14-16AWG #1/4	8-320563-1	4	1.28 \$	5.12 \$	Digi-Key	Electronics
7	Black-Oxide Alloy Steel Socket Head Screw 10-32 Thread Size, 1/2" (12.7 mm) Long	91251A342	4	0.12 \$	0.48 \$	McMaster-Carr Supply Company	Metal
8	Slotted Spring Pins 1050-1095 Spring Steel, 5 mm Diameter, 12 mm Long, for 5 mm Hole	97161A164	1	0.26 \$	0.26 \$	McMaster-Carr Supply Company	Metal
9	Alloy Steel Socket Head Screw, Black-Oxide, M4 × 0.7 mm Thread, 14 mm Long	91290A150	3	0.12 \$	0.36 \$	McMaster-Carr Supply Company	Metal
10	3D Printer Nozzle, Mk8, Brass, 0.6 mm Opening, for 1.75 mm Diameter Filament	3695N104	2	16.35 \$	32.70 \$	McMaster-Carr Supply Company	Metal
11	Button Head Hex Drive Screw, Passivated 18-8 Stainless Steel, M4 × 0.70 mm Thread, 6 mm Long	92095A188	2	0.12 \$	0.24 \$	McMaster-Carr Supply Company	Metal
12	18-8 Stainless Steel Button Head Hex Drive Screws, Black-Oxide, M4 × 0.70 mm Thread Size, 16 mm Long	97763A425	2	0.80 \$	1.60 \$	McMaster-Carr Supply Company	Metal
13	Mount base	3077 00 000 1052	1	995.00 \$	995.00 \$	Métropolitain Pop Corn Inc.	Metal & Electronics
14	Electrical-Insulating Ceramic Sleeve Washer for Number 10 Screw Size, 0.218" (5.54 mm) Overall Height	92107A418	2	3.00 \$	6.00 \$	McMaster-Carr Supply Company	Ceramic
15	Alloy Steel Flat-Tip Set Screws, Black Oxide, 1/4" (6.35 mm)-20 Thread, 3/8" (9.525 mm) Long	94105A535	4	0.24 \$	0.96 \$	McMaster-Carr Supply Company	Metal
16	Brass Hex Nut, 10-32 Thread Size	92671A195	2	0.09 \$	0.18 \$	McMaster-Carr Supply Company	Metal
17	18-8 Stainless Steel Button Head Hex Drive Screw, 10-32 Thread Size, 1-3/8" (34.93 mm) Long	92949A827	2	0.16 \$	0.32 \$	McMaster-Carr Supply Company	Metal
18	High-Temperature Ceramic fibre Pipe Insulation	4057K4	1	52.56 \$	52.56 \$	McMaster-carr Supply Company	Calcium Aluminum Silicate Ceramic fibre
19	Protection panel 36"x48"x1/25" (914.4 mm × 1219.2 mm × 1.02 mm)	8505K746	1	81.04 \$	81.04 \$	Mcmaster-Carr	Acrylic plastic
20	Cap, brush holder	42138	4	- \$	- \$	Métropolitain Pop Corn Inc.	Non-specific
21	Carbon brush	55007	4	- \$	- \$	Métropolitain Pop Corn Inc.	Non-metal
22	Machined lower spinner head	42281	1	- \$	- \$	Métropolitain Pop Corn Inc.	Non-specific
23	Machined slip ring	42126HD	2	- \$	- \$	Métropolitain Pop Corn Inc.	Metal
24	Bottom phenolic washer	20054	1	- \$	- \$	Métropolitain Pop Corn Inc.	Phenolic
25	Collector; 26" (660.4 mm) inside diameter and 9" (228.6 mm) height	42040	1	- \$	- \$	Métropolitain Pop Corn Inc.	Aluminium
26	Contact less infrared temperature sensor	WAVE-13461	1	37.96 \$	37.96 \$	Abra	Electronics
27	Black-Oxide Alloy Steel Socket Head Screw, 5/16" (7.94 mm)-18 Thread Size, 11/16" (17.46 mm) Long	90044A428	18	0.56 \$	10.08 \$	McMaster-Carr Supply Company	Metal

(continued on next page)

Table 3 (continued)

No. ARTICLE	Designator	Component	QTY	Cost per unit - currency	Total cost - currency	Supplier	Material type
28	Medium-Strength Steel Hex Nut, Grade 5, 5/16" (7.94 mm)-18 Thread Size	95505A602	18	0.1 \$	1.80 \$	McMaster-Carr Supply Company	Metal
29	U-Channel - 1/8" (3.175 mm) Wall Thickness, 3/4" (19.05 mm) High × 1" (25.4 mm) Wide × 4' (1219.2 mm) long	9001K51	2	24.33 \$	48.66 \$	McMaster-Carr Supply Company	Metal
30	304 Stainless Steel Wire Cloth, 18 × 18 Mesh Size, 0.039" (0.99 mm) Opening Size	85385T67	1	8.69 \$	8.69 \$	McMaster-Carr Supply Company	Metal
31	Alloy Steel Socket Head Screw, Black-Oxide, M2 × 0.4 mm Thread, 6 mm Long	91290A013	2	0.15 \$	0.30 \$	McMaster-Carr Supply Company	Metal
32	Steel Hex Nut, Medium-Strength, Class 8, M2 × 0.4 mm Thread	90592A075	2	0.04 \$	0.08 \$	McMaster-Carr Supply Company	Metal
33	18-8 Stainless Steel Washer for M2 Screw Size, 2.2 mm ID, 5 mm OD	93475A195	2	0.01 \$	0.02 \$	McMaster-Carr Supply Company	Metal
34	Zinc Yellow-Chromate Plated Hex Head Screw, Grade 8 Steel, 1/4" (6.35 mm)-20 Thread Size, 4" (101.6 mm) Long, Fully Threaded	92620A555	1	3.81 \$	3.81 \$	McMaster-Carr Supply Company	Metal
35	Medium-Strength Steel Serrated Flange Locknut, Grade 5, Zinc-Plated, 1/4" (6.35 mm)-20 Thread Size	99904A101	2	0.07 \$	0.14 \$	McMaster-Carr Supply Company	Metal
36	316 Stainless Steel Washer for 1/4" (6.35 mm) Screw Size, 0.281" (7.14 mm) ID, 0.625" (15.88 mm) OD	90107A029	1	0.10 \$	0.10 \$	McMaster-Carr Supply Company	Metal
37	Plywood Sheet, 1/2" (12.7 mm) Thick, 1" (25.4 mm) × 29.5" (749.3 mm)	1125T519	4	-\$	15.60 \$	McMaster-Carr Supply Company	Wood
38	Black-Oxide Alloy Steel Socket Head Screw 1/4" (6.35 mm)-20 Thread Size, 1" (25.4 mm) Long	91251A542	32	0.24 \$	7.68 \$	McMaster-Carr Supply Company	Metal
39	Medium-Strength Steel Hex Nut Grade 5, 1/4" (6.35 mm)-20 Thread Size	95505A601	32	0.07 \$	2.24 \$	McMaster-Carr Supply Company	Metal

Table 4
Bill of printable components.

No. ARTICLE	Printable	3-D printing material	QTY	Distance (mm)	Mass (g)
40	Static funnel	PLA	1	3.29	10
41	Static funnel support	PLA	1	15.04	45

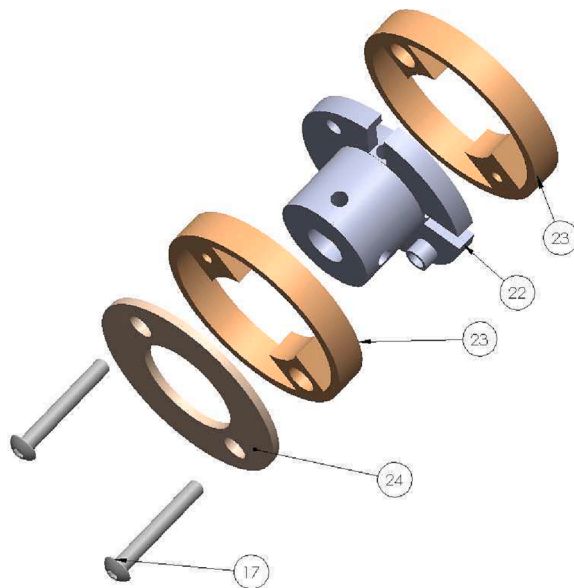


Fig. 6. Slip ring assembly. The bottom slip ring small screw hole must be aligned with the top slip ring big screw hole. .

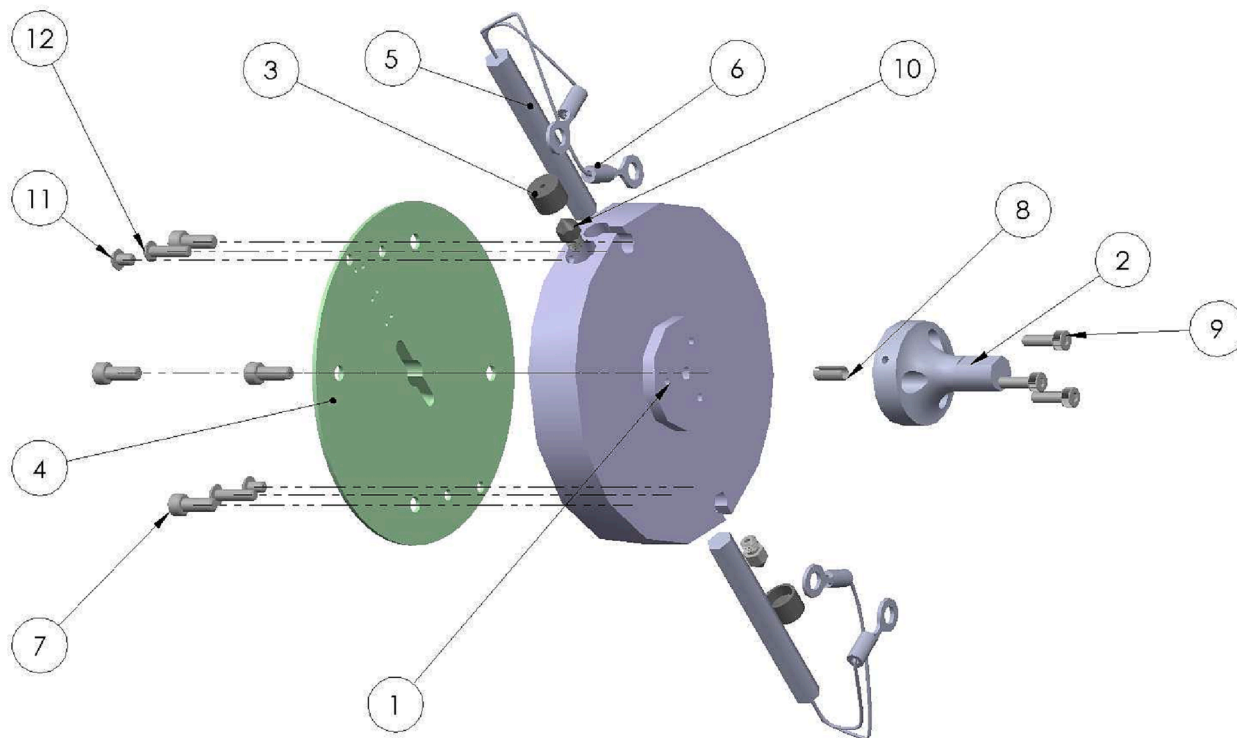


Fig. 7. Spinneret assembly: Bottom view.

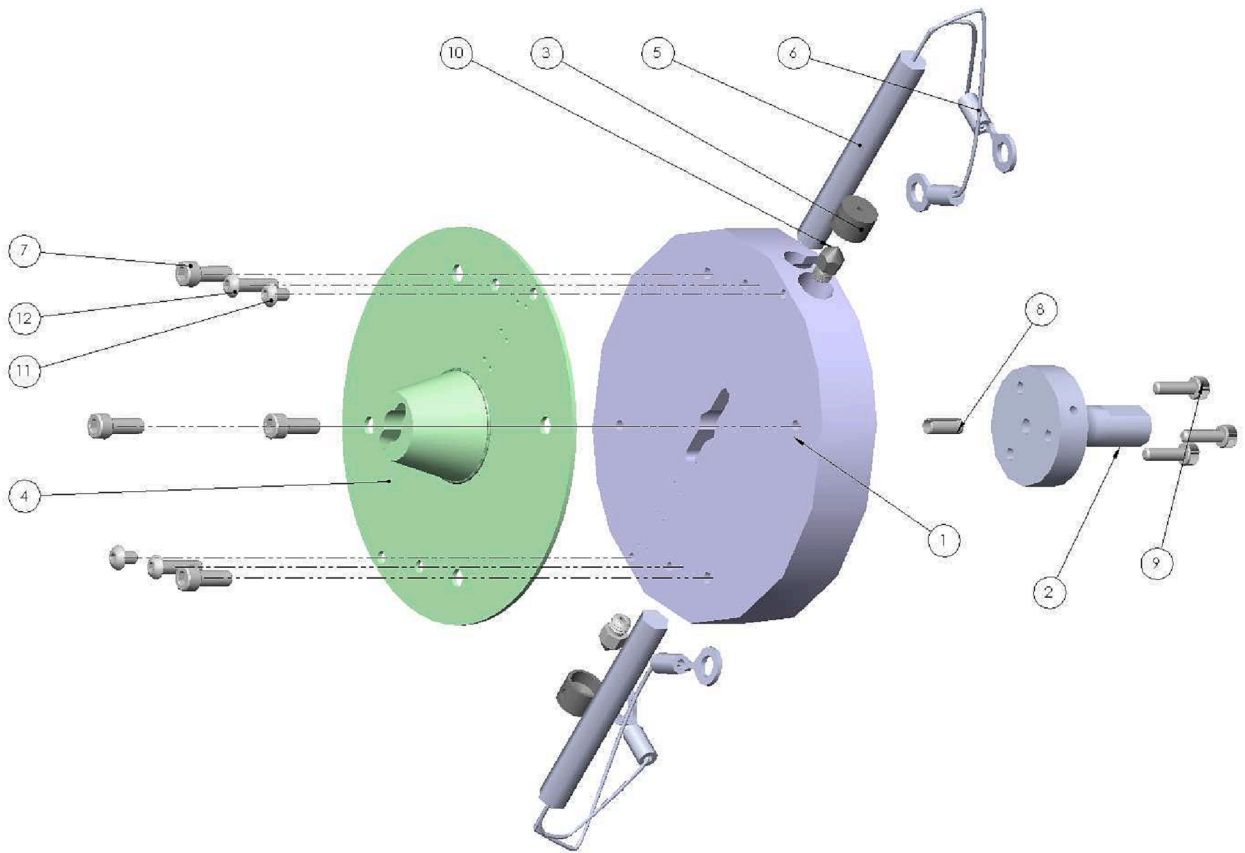


Fig. 8. Spinneret assembly: Top view.

only part that needs to be modified. Some parts from the *GoldMedalSuperflossMaxx™* machine, including the lower spinner head (Item 22), have their own article number because they are used in the build instructions and they are presented in ***bold and italic in the BOM***. The total cost for the assembly in Table 3, Table 4 and the electrical components is 2 662.16 \$.

6. Assembly instructions

Before assembling the whole spinneret, the original head has to be removed and the slip ring assembly dismantled (see Fig. 3). For more information, see pages 20 to 24 from the *GoldMedalSuperflossMaxx™* instruction manual available in the online repository [6].

6.1. Slip ring assembly

The following steps present how to assemble the slip rings. All composing elements reported here are numbered in Fig. 6:

1. Insert both slip rings (Item 23) in the lower spinner head (Item 22). To prevent short circuits, make sure that the screw hole on the lower slip ring (Item 23) is aligned with the biggest screw hole on the upper slip ring (Item 23).
2. Fix the slip rings (Item 23), the lower spinner head (Item 22) and the bottom phenolic washer (Item 24) with screws (Item 17).

6.2. Spinneret head assembly

The following steps present how to assemble the spinneret in Fig. 7 and Fig. 8:

1. Insert the spring pins (Item 8) inside the spinneret head (Item 1) with a hammer.
2. Insert the spring pins (Item 8) in the head support (Item 2). Make sure the three M4 thread holes for the screws (Item 9) are aligned with the spinneret head (Item 1) and support (Item 2). Use a hammer if the spring pins (Item 8) are not fully inside the head support (Item 2).
3. Fix the spinneret head (Item 1) and support (Item 2) with the screws (Item 9).
4. Screw the nozzle (Item 10) inside the spinneret (Item 1) M6 threaded hole and tighten it with a ratchet.

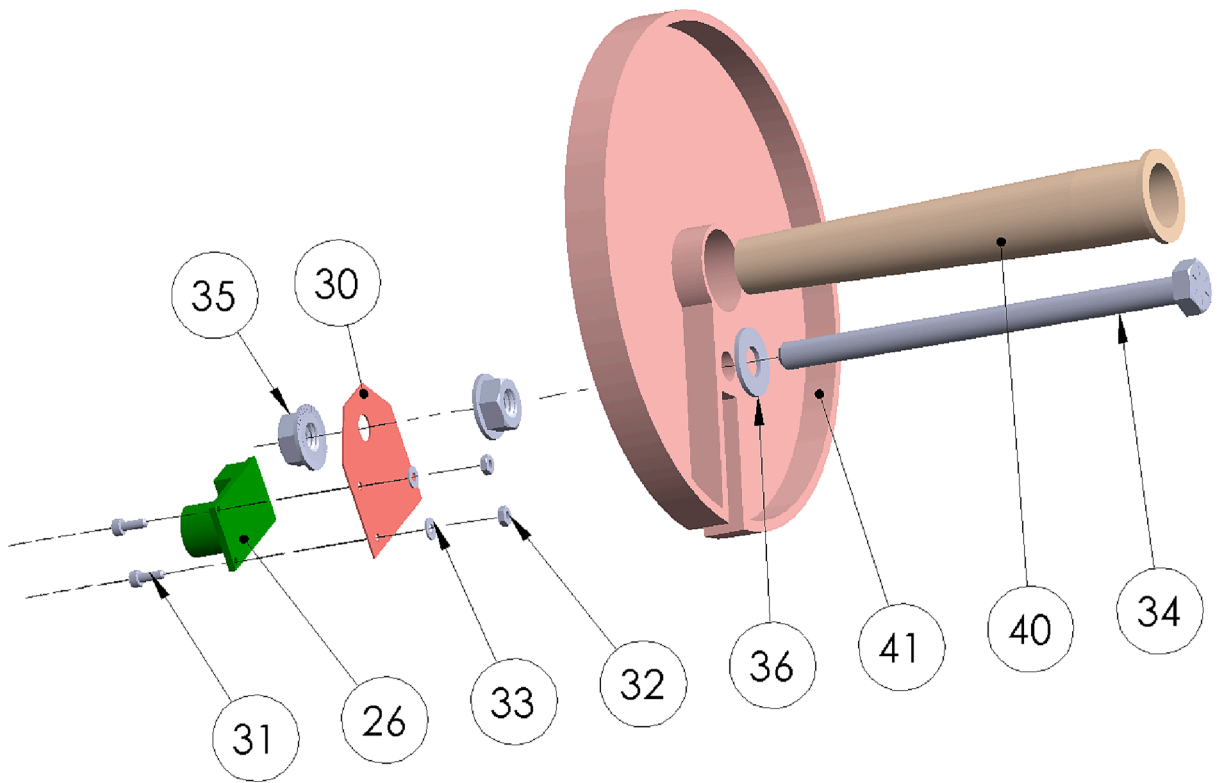


Fig. 9. Spinneret assembly: Infrared Sensor assembly.

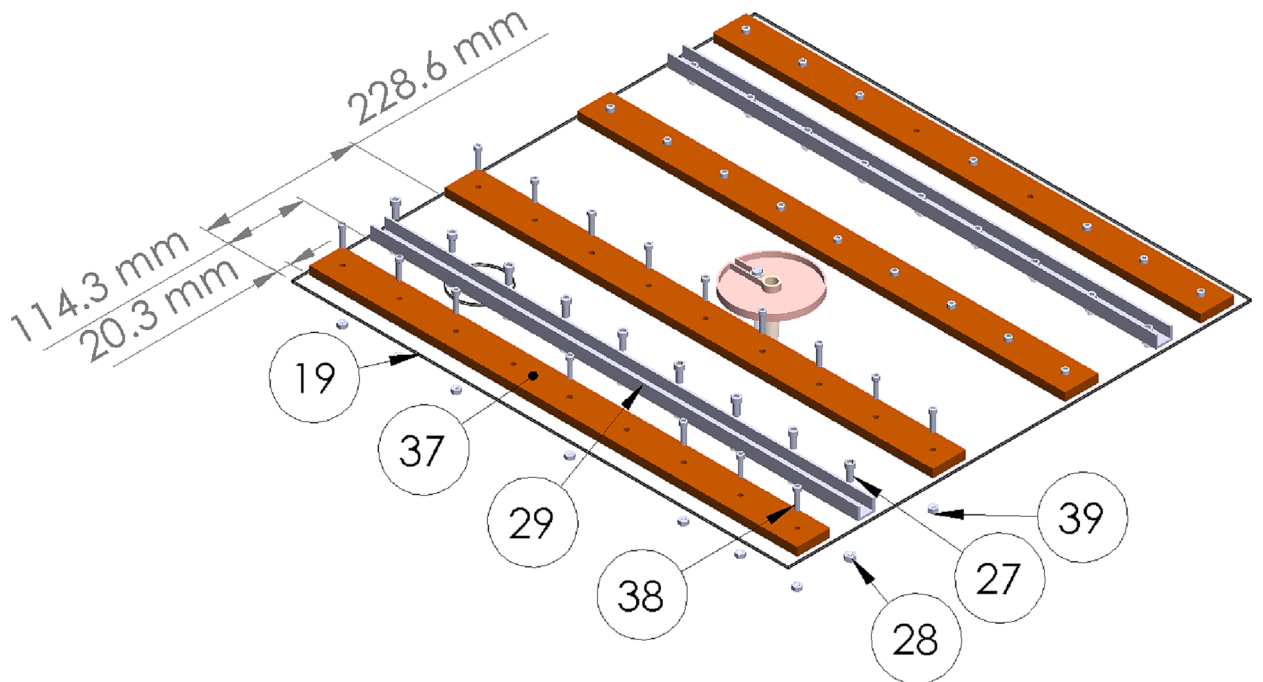


Fig. 10. Protection panel assembly.

5. Insert the plug (Item 3) in this same hole. Note that this plug is optional as it is used to reduce fibre dislocation at the exit of the nozzle but no notable differences in the fibre quality were seen with or without it. Also, removing the plugs is difficult due to thermal expansion during heating.
6. Align the plug (Item 3) pocket with the spinneret (Item 1) M4 hole above the M6 thread hole.
7. Repeat steps 4 to 6 with the second nozzle (Item 10) and plug (Item 3).
8. Place the funnel (Item 4) above the spinneret (Item 1) and align their holes.
9. Fix the plugs (Item 3) and the funnel (Item 4) with screws (Item 11). This will prevent the plugs (Item 3) from being ejected during operation.
10. Fix the funnel (Item 4) and the spinneret head (Item 1) with screws (Item 7).
11. Insert one heating cartridge (Item 5) inside the spinneret head (Item 1). Make sure the cartridge (Item 5) wires were cut at the required length (± 3.5 in) and crimped to the ring connectors (Item 6). Be careful to keep the wires under the spinneret head (Item 1) to avoid fibres from hitting them. Apply isolation tissue around the heating cartridge (Item 5) wires to protect them from short circuits.
12. Fix the cartridge (Item 5) with the screws (Item 12). It prevents them (Item 5) from being ejected during operation.
13. Repeat steps 11 and 12 with the second cartridge (Item 5).

6.3. Infrared sensor assembly

The following steps present how to assemble the infrared sensor in Fig. 9:

1. Insert the screw (Item 34) and the washer (Item 36) through the support (Item 41).
2. Fix the first flange locknut (Item 35) 0.5 inches (12.7 mm) away from the tip of the screw (Item 34).
3. Insert the screw (Item 34) through the wire cloth (Item 30) and fix them with the second flange locknut (Item 35). The wire cloth (Item 30) must be tightly pressed between both locknuts (Item 35).
4. Fix the infrared sensor (Item 26) and the wire cloth (Item 30) with the screws (Item 31), washers (Item 33) and nuts (Item 32).
5. Insert the static funnel (Item 40) through the support (Item 41).

To accurately read the temperature, verify if the IR sensor lens (Item 26) is pointing towards the spinneret's flat surface around the rotating funnel (Item 4). The sensor should not be more than 15 cm away from the spinneret because it will be less accurate in reading the temperature.

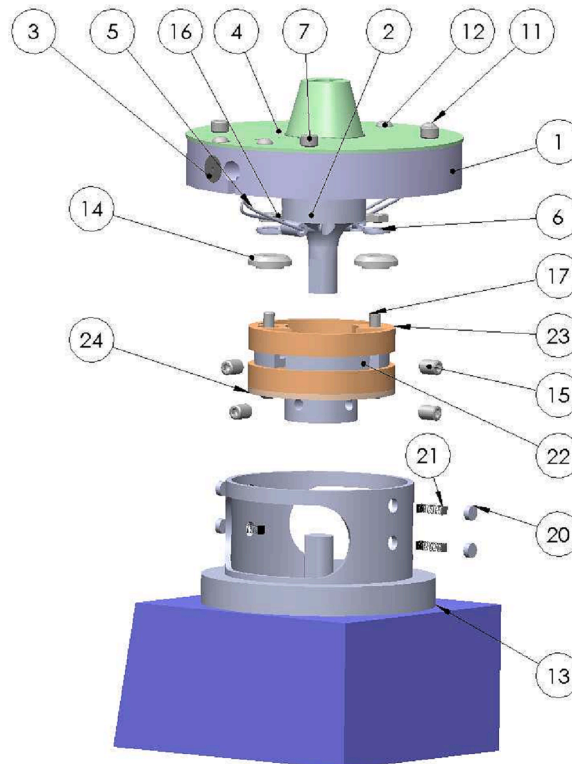


Fig. 11. Spinneret body assembly.

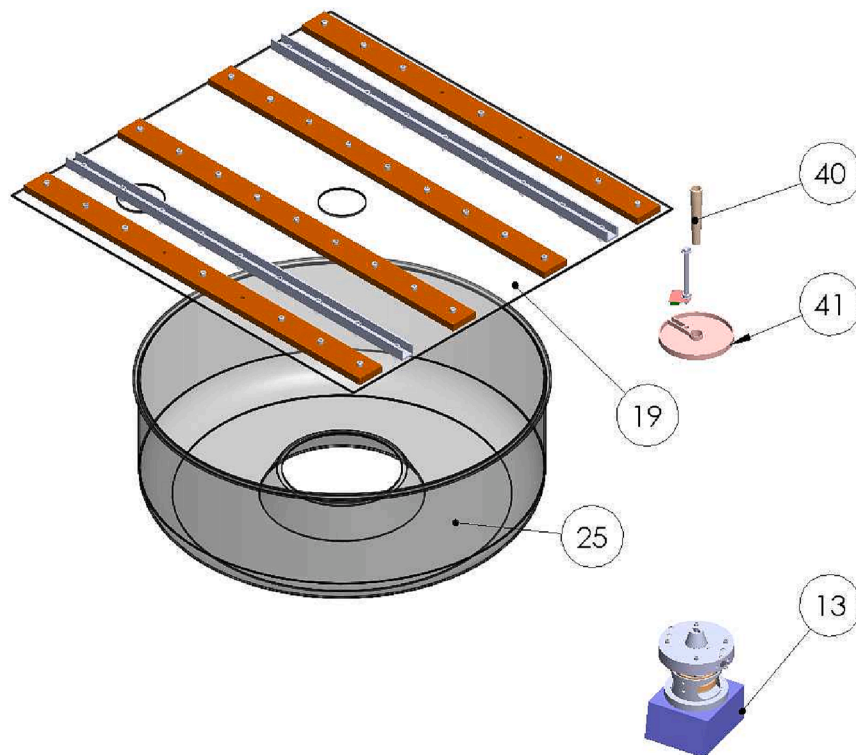


Fig. 12. Overall assembly.

6.4. Protection panel assembly

The following steps present how to assemble the protection panel presented in Fig. 10:

1. Place the first wood panel (Item 37) on the protection panel (Item 19) at the indicated distance presented in Fig. 10.
2. Fix the wood panel (Item 37) and the protection panel (Item 19) to the screws (Item 38) with nuts (Item 39).
3. Repeat the previous steps with the second wood panel (Item 37) while respecting the indicated distance presented in Fig. 10.
4. Place the U channel (Item 29) on the protection panel (Item 19) at the indicated distance presented in Fig. 10.
5. Fix the U channel (Item 29) and the protection panel (Item 19) to the screws (Item 27) with nuts (Item 28).
6. Repeat the previous steps with the remaining components on the opposite side of the static funnel support (Item 41). The assembly is symmetrical to the static funnel (Item 41).

6.5. Spinneret body assembly

The following steps present how to assemble the spinneret and slip ring assembly to the *GoldMedalSuperflossMaxx™* body and refer to Fig. 11 and Fig. 12):

1. Place the washers (Item 14) on the screws (Item 17) from the slip ring assembly in Section 6.1.
2. Insert the spinneret assembly from Section 6.2 into the slip ring assembly from Section 6.1.
3. Place the cartridge ring connectors (Item 6) from the spinneret assembly in Section 6.2 on the screws (Item 17). There must be one connector at each screw per cartridge to create a parallel circuit.
4. Fix the cartridge ring connectors (Item 6) to the screws (Item 17) with nuts (Item 15).
5. Fix the spinneret assembly from Section 6.2 to the lower spinner head (Item 22) with the upper set screws (Item 15).
6. Be sure that the base (Item 13) position is locked. Insert the slip ring assembly from Section 6.1 in the base (Item 13).
7. Fix the lower spinner head from the slip ring assembly in Section 6.1 to the base (Item 13) with the bottom set screws (Item 15).
8. Insert the carbon brushes (Item 21) in the base (Item 13). Check that they touch both slip rings.
9. Fix the carbon brushes (Item 21) with the brush holders (Item 20).
10. Place the collector on the base (Item 13).
11. Place the protection panel assembly from Section 6.4 on the collector (Item 25).
12. Place the support (Item 41) and the 3D printed funnel (Item 40) at the center of the protection panel (Item 19)

7. Operating instructions

7.1. Safety precautions

Before starting the machine, some safety validations are required. Make sure that the emergency button is activated at all times while doing the first 3 steps. Steps 1 to 3 must be carried out without the collector and the protection panel.

1. Verify the spinneret stability with a surface sensor. Alternatively, it is also possible to use a bubble level. If the surface is not levelled, check all mounting operations for possible mistakes. Repeat this step after each experiment.
2. Verify the electrical resistance between the spinneret and the heater electrical wires with a multimeter. Use the instrument on one of the ring connectors (Item 6) and either the spinneret head (Item 1) or the funnel (Item 4). If the resistance is not $\pm 14 \Omega$, dismantle the spinneret and check if the cartridges are damaged. Also, no metallic objects except the ones from the build instructions must come in contact with the spinneret during fibre production because there is an electrical connection between it and the cartridges.
3. Check by rotating manually the spinneret that the cartridge wires stay under the spinneret and that they do not rub on anything. Additionally, check all electrical connections: this must be done before each experiment.
4. Turn on the motor while the heating switch remains off and check the current with a clamp meter. The motor current must be ± 1.5 A.
5. Turn on the motor and the heater and check the heater current. The corresponding resistance and power that can be calculated must be close to the theoretical values indicated by the manufacturer.

7.2. Fibre production with the funnel

1. Activate the ventilation system.
2. Deactivate the emergency button.
3. Activate the motor.
4. Set the rheostat at 100–110 V and activate it.
5. Preheat the spinneret for ± 8 min or until 200°C is measured by using a heat sensor. If the spinneret temperature is over 230°C, lower the voltage. The temperature of 200°C has been chosen for the polypropylene (PP) or polylactide (PLA) pellets presented in [Table 5](#).
6. Pour 1/8 teaspoon of pellets in the spinneret and wait until enough fibres are produced before adding more pellets. Do not add more than 1/8 teaspoon of pellets because the funnel will be overfilled.
7. Remove the static funnel (Item 40) after filling the spinneret to avoid melting it.

Since the density of the pellets vary between polymers, it is recommended to not pour more than 1/8 teaspoon of pellets in the spinneret at a time.

7.3. Fibre production without the funnel

The following steps to produce fibres without the funnel are slightly changing from the ones presented in Section 7.2. The main difference is that the spinneret needs to be pre-filled with pellets before preheating and activating the motor.

1. Activate the ventilation system.
2. Pour 1/8 teaspoon of pellets inside the spinneret.
3. Deactivate the emergency button.
4. Set the rheostat at 100–110 V and activate it.
5. Preheat the spinneret for ± 3 min or until 200°C is measured by using a heat sensor.
6. Activate the motor as soon as the spinneret reaches 200°C to avoid polymer degradation. The temperature of 200°C has been chosen for the polypropylene (PP) or polylactide (PLA) pellets presented in [Table 5](#). Note that the polymer melts quickly when the motor is off and might be degrading if its degradation temperature is close to the process temperature. Thus, it is recommend to not exceed 230°C regardless of the polymer.

For Section 7.2 and 7.3, PP and PLA of any melt flow index (MFI) can produce fibres with a heating temperature of 200°C. However, most polymers of MFI lower than 16 g/10 min (which means high viscosity) did not produce as much fibres as those of higher MFI with the same amount of pellets poured into the spinneret. This means that the heating temperature needs to be increased when using polymers of lower MFI. The optimal heating temperature to extrude polymers of a specific MFI is determined through experimentation at different heating temperatures and then analyzing the fibres morphology through scanning electron microscopy (SEM). Overheating is not an issue when using the funnel in Section 7.2 because the polymer melt is extruded once its viscosity is low enough. Raghavan et al. [20] studied fibres produced through hot melt CS and analyzed the degradation of PP pellets and fibres of MFI ranging from 36 g/10 min to 1550 g/10 min through thermogravimetric analysis (TGA). Their results shown that molecular weight loss began at 400°C,

thus degradation should not be an issue when producing fibres with PP. However, it is still recommended to analyze polymer fibres degradation because their mechanical properties such as tensile strength can be impacted.

7.4. Ending process

For safety measures, fibres can only be collected by following these steps after Section 7.2 or 7.3:

1. Keep heating the spinneret at 200°C between 5 and 10 min without adding pellets, then close the rheostat.
2. Wait until the temperature of the spinneret reaches 35°C before shutting off the motor. Spinneret cooling takes up to 20 min.
3. Shut off the motor.
4. Activate the emergency button.
5. Remove the protective cover and the static support (Item 41).
6. Collect fibres with a clean wooden stick.
7. Close the ventilation system.

7.5. Maintenance and preventive inspections

- Make sure there is no current leakage between the spinneret and the electrical cartridges before AND during production.
- Buy spare heating cartridges in case of damage. The heating cartridges are the most fragile components of this apparatus because their wires end up burning. Normally, the wires need to stay away from the heating object, but it is not possible with this apparatus. Also, the cartridge efficiency may decrease over time.
- Add insulating tape around the heating cartridge wires and renew them when needed.
- To remove the heating cartridges from the spinneret, use a tool similar to an Allen key to push them out. Do not pull out the heating cartridges because the wires will break.
- Before starting an experiment, the measured temperature from the IR sensor should be compared with the IR camera. The measured temperature between both tools is usually similar, but the IR sensor can be 8°C less precise than the IR camera.

8. Validation and characterization

8.1. Design choices

- Machine: The *GoldMedalSuperflossMaxx™* cotton candy machine was chosen because of its availability and its safe operation process.
- Spinneret head: The spinneret head was designed for customization. Indeed, the nozzles are interchangeable. Then, it is possible to feed the spinneret continuously using the funnel. Thermocouples may also be installed in the spinneret head for easy temperature reading. Since the apparatus is used in a scientific environment, fibre production rate is not a critical aspect. For this reason, the number of channels was limited to two. In addition, the heating cartridges were chosen to facilitate their installation and to unify the heating distribution around the spinneret.
- Collector: The same collector from the *GoldMedalSuperflossMaxx™* machine is used for the hardware as it is efficient to protect the user from the rotating spinneret. It is possible to build a custom collector, but in any case, it is recommended to build an enclosure system around the hardware for safety measures.
- Panel: The panel is used to reduce heat loss between the spinneret and the collector. It's important to control the temperature outside the spinneret because it reduces clogging at the nozzle's tip. The panel also protects the user from polymer droplet ejections and it allows the user to safely feed the spinneret during rotation. The shape of the panel can be circular as long as it covers the collector and the reinforcements are adapted to the new shape. The panel was also designed to support the static funnel.

8.2. Capabilities, limitations and issues of the hardware

8.2.1. Capabilities

- Hardware designed to produce fibres with polymer melt: It would also be possible to use polymer solution.
- Versatile design: The design of the hardware is versatile enough to try different extrusion geometries with melt.
- Cleaning: At the end of an experiment, with the motor ON, simply preheat the spinneret at a temperature above the extruded polymer melting point. Wait for a few minutes for the remaining polymer melt inside the spinneret to be completely extruded.
- Heating: The heating cartridges can produce up to a 1000 W when connected in parallel and it can preheat the spinneret up to 300°C at 110 V.

8.2.2. Limitations

- Production rate: With only two channels allowing the passage of polymer flow, the production rate is low. However, the purpose of this hardware is to further understand fibre formation from molten polymer. Assembling the funnel on the spinneret head increases the production rate since adding polymer pellets during production is possible.
- Filling capacity: It is not possible to produce large quantities of fibres as the spinnerets reservoir can contain up to 2.13cm^3 , but adding the funnel helps to fill it continuously.
- Heating capacity: The maximum obtainable temperature depends on the heating power of the cartridges. Stronger heating cartridges can be purchased if the heating capacity is insufficient.

8.2.3. Issues

- Aerodynamic cooling: Cooling the spinneret between experiments could take up to 10 min, even when the motor is turned on and the panel removed. Cooling takes up to 20 min when the panel is not removed.
- Clogging: There can be some clogging inside the channels and the nozzles. To remove the clogs, preheat the spinneret until it reaches $\pm 215^\circ\text{C}$ and activates the motor. If the parts are still clogged, heat them with a heat gun. In this work, the heat gun was never used, so appropriate heat control reduces risks of clogging.
- Fibre accumulation under the spinneret: If the heating cartridges' wires are longer than the recommended length, they may overlap the spinneret during production and collect some fibres.
- Heating cartridge damage: The heating cartridges' wires can be damaged if not properly insulated or if the cartridge is pulled out from the spinneret instead of being pushed out.
- The head support (Item 2) deforms with time. Thus, more vibrations were observed while producing fibres or switching OFF the motor, so machining a spare head support is recommended.
- Burnt fibres were observed when the rotating funnel was not used because of the rapid temperature increase during pre-heating. Thus, it is recommended to carefully monitor the spinneret temperature if it is heated higher than 200°C . Regardless of the spinneret feeding method, heating it at a temperature lower than the polymer degradation point is recommended.

8.3. Temperature distribution and range

The temperature on the top surface of the spinneret was $\pm 42^\circ\text{C}$ higher than at its lateral surface. To compare the temperature between the surfaces, an infrared camera was used. It is important to note that the temperature at both the top and the lateral surfaces of the spinneret was the same with the motor OFF.

8.4. Fibre quality analysis

While scanning electron microscopy (SEM) was used to analyze fibre quality and diameter distribution in Section 8.5, the following fibre characterization methods should be used further evaluate fibre quality: X-ray diffraction (XDR), Fourier-transform infrared spectroscopy (FTIR), tensile test and surface area measurement [21].

8.5. Relevant use cases

This section presents three use cases of fibre production using the nozzle configuration with an inner diameter of 0.6 mm (see Fig. 4a) where the spinneret rotating speed is 3450 rpm. It is important to mention that the optimal processing parameters such as the heating temperatures were not determined here because it was not the objective of this work. In the first two use cases, PP with an MFI of 12.4 g/10 min in powder form and PLA filaments used in 3d printing were used. The PLA filaments were cut into pellets. The rotating funnel was not used here, so the pellets were pre-poured in the spinneret before preheating them for 3 min up to 200°C for PP and 230°C for PLA. Then, the motor was activated while heating the spinneret and the fibres were produced at 250°C for PP and 280°C for PLA. In the third use case, PP pellets with an MFI of 127 g/10 min were used with the rotating funnel so it was possible to pour the pellets in the spinneret while it was heating and rotating. Preheating the spinneret up to 200°C before pouring the pellets took 5 min. Four to six pellets at a time were poured in the spinneret during fibre production until the heating temperature of 250°C was measured.

The glass transition (T_g) and melting temperature (T_m), MFI, density and supplier for each polymer used in the use cases are

Table 5

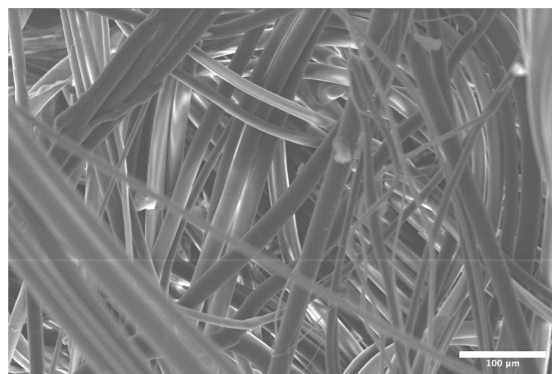
Data of the tested polymers in the use cases.

Material	T_g [$^\circ\text{C}$]	T_m [$^\circ\text{C}$]	MFI [g/10 min]	Density [kg/m ³]	Supplier
Polypropylene (PP)	-15[26]	140[26] to 200	12.4	900	Pro-fax 6323 from Lyondellbasell
PP	-15[26]	140[26] to 200	127 ^a	130 ^a	NA
Poly lactide (PLA)	55 to 75[26]	164 to 178[26]	16	1240	ECOMAX [®] PLA 3D printing filament from 3DXTECH

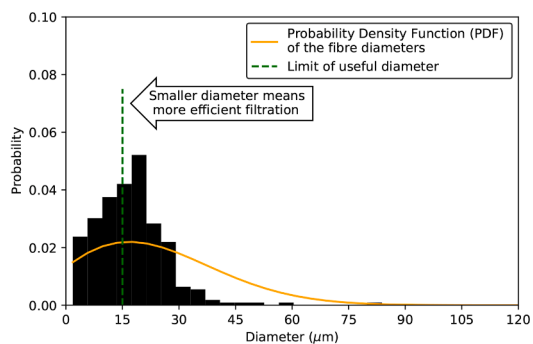
^a The specific MFI of this PP was not known either, so our research team measured it with the melt flow index equipment and obtained 127 g/10 min. All measures for the weight, diameter and MFI were repeated twice.

Table 6
Fibre diameter measurements.

Polymer	MFI [g/10 min]	Mean \pm s.d. [μ m]
PP	127	9 \pm 8.31
PLA	16	16.16 \pm 9.30
PP	12.4	23.80 \pm 18.07

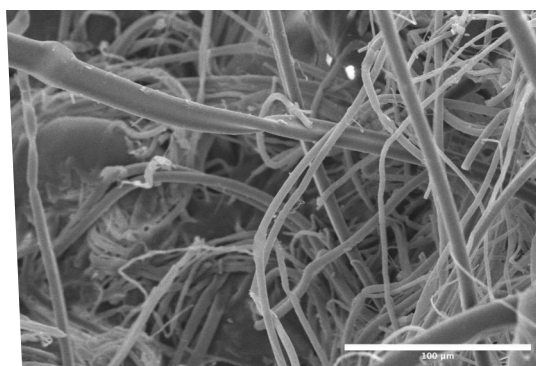


(a)

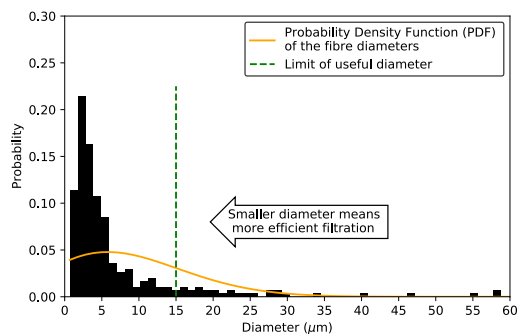


(b)

Fig. 13. SEM image (a) and Rayleigh distribution curve (b) of PP fibres with an MFI of 12.4 g/10 min - Discontinuous feeding.

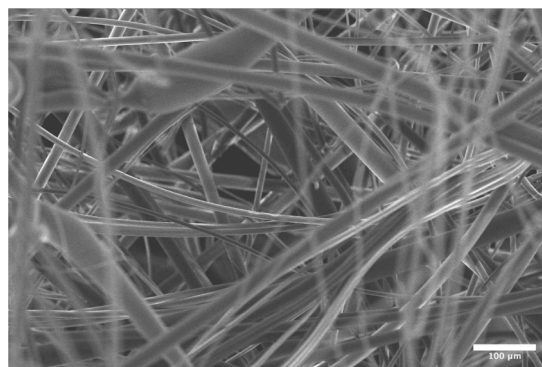


(a)

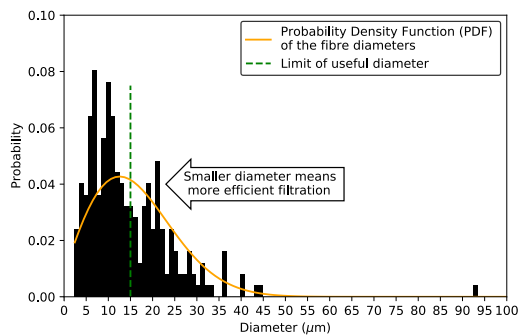


(b)

Fig. 14. SEM image (a) and Rayleigh distribution curve (b) of PP fibres with an MFI of 127 g/10 min - Continuous feeding.



(a)



(b)

Fig. 15. SEM image (a) and Rayleigh distribution curve (b) of PLA fibres with an MFI of 16 g/10 min - Discontinuous feeding.

presented in Table 5. Polypropylene is commonly used for studies in hot melt CS and is selected here as well [22,20,23]. Previous studies did not lead to a common conclusion as to the appropriate viscosity of PP, which is evaluated with its MFI or molecular weight, when producing fibres in this process because a too low viscosity after melt extrusion results in jet breaks [22]. Thus, our research team was interested in comparing the fibres diameter and morphology between lower MFI (high viscosity) and higher MFI (low viscosity) PP. The second polymer, PLA, was used to analyze biodegradable fibres in future work.

The quality of the fibres is evaluated by the size of their diameter and the formation of beads. Since a smaller fibre diameter is better to filtrate air particles [24], 15 μm was our limit of acceptable diameter size. This limit was determined by measuring the diameter of the fibres in the filtering layer of a medical mask. The average fibre diameter measured was between 2 and 3 μm and the largest ones were $\pm 15 \mu\text{m}$. As a comparison with melt-blown, Drabek & al. reported that fibre diameters were between 2 and 7 μm with fibres as large as 30 μm [25]. The surface area of the pores between the fibres can be measured using the *ImageJ* software [21]. Reducing the pores area increases filtration efficiency because more aerosols will be captured by the fibres, but no results were obtained because of the important amount of depth between fibres. Areal weight is another fibre property in filtration, but it will not be evaluated in this work.

The fibres were analyzed with the *S3600-N Hitachi* SEM after coating them with the *Gold Sputter Coating K550X* for 2 min with a coating current of 25 mA. Minimum three SEM images were used to measure the fibres through *ImageJ*, leading to 150–290 measurements in total.

8.5.1. Results and discussion

The fibre diameter mean and standard deviation (s.d.) are presented in Table 6 for each studied polymer. Fig. 13a and b present an SEM image and the Rayleigh distribution curve of PP fibres with an MFI of 12.4 g/10 min. The rotating funnel was not used in this test, but no burnt fibres were observed.

Fig. 14a and b present an SEM image and the Rayleigh distribution curve of PP fibres with an MFI of 127 g/10 min. The rotating funnel was used in this test.

The diameter distribution curve of PP fibres with an MFI of 12.4 g/10 min in Fig. 13b is larger than the curve from the MFI of 127 g/10 min in Fig. 14b. Indeed, while the mean and s.d. for PP fibres with an MFI of 12.4 g/10 min are $23.80 \pm 18.07 \mu\text{m}$ (Table 6), those produced with an MFI of 127 g/10 min measured $9 \pm 8.31 \mu\text{m}$ (Table 6), which is much smaller. The studies that produced PP fibres through hot melt CS measured an average diameter of 0.5–9.08 μm [20,22,8,23,27], thus our results for the MFI of 127 g/10 min are in this bracket.

Less beaded and broken fibres for the MFI of 12.4 g/10 min in Fig. 13a than the fibres for the MFI of 127 g/10 min in Fig 14a were observed. A possible explanation could be that the viscosity of the jet was too low at an MFI of 127 g/10 min when heating the spinneret up to 250°C. Consequently, the jet broke and beaded fibres were formed because the viscous force was not high enough to oppose the centrifugal force. Thus, the heating temperature should be reduced when producing PP fibres of high MFI.

Fig. 15 and b present an SEM image and the Rayleigh distribution curve of PLA fibres with an MFI of 16 g/10 min. The rotating funnel was not used in this test, but no burnt fibres were observed.

The average PLA fibre diameter measured is $16.16 \pm 9.30 \mu\text{m}$ (Table 6) and no beads were observed in Fig. 15a. To the authors knowledge, only Ref. [28] produced PLA fibres and they varied between 10–50 μm and 0.993 μm as their smallest diameter, which means it is too early to assume that these diameters are common for PLA. PLA fibres produced smaller and more uniform fibres than PP fibres with an MFI of 12.4 g/10 min (Table 6), suggesting that increasing the MFI reduces fibre diameter.

9. Conclusion

In summary, a versatile hot melt CS apparatus was designed in this work. Indeed, different extrusion geometries such as the nozzle and nozzlefree geometries can be used. The desired heating temperature can be maintained through PID by using the IR sensor. With the rotating funnel, polymer pellets of any kind can be easily poured inside the spinneret during production. In future work the influence of MFI on PP fibres by using this apparatus will be analyzed.

CRediT authorship contribution statement

Jason Gunther: Conceptualization, Methodology, Validation, Formal analysis, Investigation, Writing - original draft, Visualization. **Jacques Lengaigne:** Conceptualization, Methodology, Software, Validation, Formal analysis, Investigation, Data curation, Writing - review & editing, Supervision, Project administration. **Mélanie Girard:** Validation, Writing - review & editing. **Valérie Toupin-Guay:** Conceptualization, Methodology, Software, Formal analysis, Investigation. **James T. Teasdale:** Conceptualization. **Martine Dubé:** Writing - review & editing, Resources. **Ilyass Tabiai:** Writing - review & editing, Resources.

Declaration of Competing Interest

The authors declare that they have no known competing financial interests or personal relationships that could have appeared to influence the work reported in this paper.

Acknowledgements

The authors appreciate the help from Nabil Mazeghrane, Alain Grimard, Michel Drouin, Serge Plamondon, Adam Smith, Joël Grignon and Mario Corbin from the mechanical engineering department at École de Technologie Supérieure for fabricating and welding the parts, programming and electrical management validation of the apparatus and their overall feedback through the design of the apparatus and this article. The authors thank Supermax Healthcare Canada and MITACS Accelerate for funding this research project.

References

- [1] G. Medal, Gold Medal 2022 concession equipment and supplies catalog (2022). URL:<https://www.gmpopcorn.com/Portals/0/Catalog/2022/index.html>.
- [2] J.J. Rogalski, C.W.M. Bastiaansen, T. Peijs, Rotary jet spinning review – a potential high yield future for polymer nanofibers, *Nanocomposites* 3 (4) (2017) 97–121, <https://doi.org/10.1080/20550324.2017.1393919>. URL: <https://www.tandfonline.com/doi/full/10.1080/20550324.2017.1393919>.
- [3] E. Stojanovska, M. Kurtulus, A. Abdelgawad, Z. Candan, A. Kilic, Developing lignin-based bio-nanofibers by centrifugal spinning technique, *Int. J. Biol. Macromol.* 113 (2018) 98–105, <https://doi.org/10.1016/j.ijbiomac.2018.02.047>. URL: <http://www.sciencedirect.com/science/article/pii/S0141813017346299>.
- [4] N. Trade, CYCLONE PILOT G1, consulted on 05/12/22 (2023). URL:<https://www.nano4fibers.com/we-sell>.
- [5] M. Rihova, A.E. Ince, V. Cimančova, L. Hromadko, K. Castkova, D. Pavlinak, L. Vojtova, J.M. Macak, Water-born 3D nanofiber mats using cost-effective centrifugal spinning: comparison with electrospinning process: A complex study, *J. Appl. Polym. Sci.* 138 (5) (2021) 49975, <https://doi.org/10.1002/app.49975>. URL: <https://onlinelibrary.wiley.com/doi/abs/10.1002/app.49975>.
- [6] J. Gunther, M. Girard, I. Tabiai, Hot melt centrifugal spinning apparatus for thermoplastic micro- and nano-fibres production, OSF, publisher, Nov. 2022, [10.17605/OSF.IO/JH6QY](https://doi.org/10.17605/OSF.IO/JH6QY).
- [7] Z.-M. Zhang, Y.-S. Duan, Q. Xu, B. Zhang, A review on nanofiber fabrication with the effect of high-speed centrifugal force field, *J. Eng. Fibers Fabr.* 14 (2019) 11, <https://doi.org/10.1177/1558925019867517>. URL: <http://journals.sagepub.com/doi/10.1177/1558925019867517>.
- [8] R. Wongpajan, S. Thumsorn, H. Inoya, M. Okoshi, H. Hamada, Development of Cotton Candy Method for High Productivity Polypropylene Fibers Webs, *Fibers and Polymers* 19 (1) (2018) 135–146, <https://doi.org/10.1007/s12221-018-7574-0>. URL: <http://link.springer.com/10.1007/s12221-018-7574-0>.
- [9] A. Kilic, Areka's Centrifugal Spinning System, 2018. URL:https://www.researchgate.net/publication/325923847_Areka's_Centrifugal_Spinning_System.
- [10] M. Rajendran, Optimization Of A Centrifugal Spinning Machine, *ScienceOpen Preprints* (2021) 21Publisher: ScienceOpen. doi:10.14293/S2199-1006.1.SOR-PPULVZA.v1. URL:<https://www.scienceopen.com/hosted-document?doi=10.14293/S2199-1006.1.SOR-PPULVZA.v1>.
- [11] S. Suttiruangwong, W. Rodchanasuripron, A. Duangjan, S. Srisamut, M. Seadan, Y. Baimark, Non-woven Poly (Lactic Acid) Fibers Prepared by Rotary Jet Spinning Technique, Kyoto, Japan, 2018.
- [12] I. Sebe, B. Kállai-Szabó, I. Oldal, L. Zsidai, R. Zelkó, Development of laboratory-scale high-speed rotary devices for a potential pharmaceutical microfibre drug delivery platform, *Int. J. Pharm.* 588 (2020), 119740, <https://doi.org/10.1016/j.ijpharm.2020.119740>. URL: <https://www.sciencedirect.com/science/article/pii/S0378517320307249>.
- [13] J.E. Domínguez, E. Olivos, C. Vázquez, J.M. Rivera, R. Hernández-Cortes, J. González-Benito, Automated low-cost device to produce sub-micrometric polymer fibers based on blow spun method, *HardwareX* 10 (2021), e00218, <https://doi.org/10.1016/j.ohx.2021.e00218>. URL: <https://www.sciencedirect.com/science/article/pii/S246806722100047X>.
- [14] A.N. Mitropoulos, K.T. Kiesewetter, E. Horne, J. Butler, J.R. Loverde, J.K. Wickiser, Uniform wet-Spinning Mechanically Automated (USMA) fiber device, *HardwareX* 8 (2020), e00124, <https://doi.org/10.1016/j.ohx.2020.e00124>. URL: <https://www.sciencedirect.com/science/article/pii/S246806722030033X>.
- [15] J. Huang, V. Koutsos, N. Radacsi, Low-cost FDM 3D-printed modular electro-spray–electrospinning setup for biomedical applications, *3D Printing in Medicine* 6 (1) (2020) 8, <https://doi.org/10.1186/s41205-020-00060-x>. URL: <https://threedmedprint.biomedcentral.com/articles/10.1186/s41205-020-00060-x>.
- [16] A. Spataru, Serial-Studio/Serial-Studio: Multi-purpose serial data visualization & processing program (2020). URL:<https://github.com/Serial-Studio/Serial-Studio>.
- [17] N.E. Zander, Formation of melt and solution spun polycaprolactone fibers by centrifugal spinning, *J. Appl. Polym. Sci.* 132 (2) (2015) 9, <https://doi.org/10.1002/app.41269>. URL: <https://onlinelibrary.wiley.com/doi/abs/10.1002/app.41269>.
- [18] M.R. Badrossamay, H.A. McIlwee, J.A. Goss, K.K. Parker, Nanofiber Assembly by Rotary Jet-Spinning, *Nano Lett.* 10 (6) (2010) 2257–2261, <https://doi.org/10.1021/nl101355x>. URL: <https://www.ncbi.nlm.nih.gov/pmc/articles/PMC3704151/>.
- [19] R. Rangkupan, D. Reneker, Electrospinning Process of Molten Polypropylene in Vacuum, *J. Met. Mater. Miner.* 12 (2003), 8, journal site: <https://www.jmmm.material.chula.ac.th/index.php/jmmm/article/view/1290>. URL: https://www.researchgate.net/publication/237661894_Electrospinning_Process_of_Molten_Polypropylene_in_Vacuum.
- [20] B. Raghavan, H. Soto, K. Lozano, Fabrication of Melt Spun Polypropylene Nanofibers by Forcespinning, *J. Eng. Fibers Fabr.* 8 (1) (2013), <https://doi.org/10.1177/155892501300800106>, 1558925013008000. URL: <http://journals.sagepub.com/doi/10.1177/155892501300800106>.
- [21] I.D. Wijayanti, A.K. Saputra, F. Ibrahim, A. Rasyida, P. Suwarta, I. Sidharta, An ultra-low-cost and adjustable in-house electrospinning machine to produce PVA nanofiber, *HardwareX* 11 (2022), e00315, <https://doi.org/10.1016/j.ohx.2022.e00315>. URL: <https://www.sciencedirect.com/science/article/pii/S2468067222000608>.
- [22] M.M. Bandi, Electrocharged facepiece respirator fabrics using common materials, *Proc. R. Soc. A: Math., Phys. Eng. Sci.* 476 (2243) (2020) 20200469, publisher: Royal Society. doi:10.1098/rspa.2020.0469. URL:<https://royalsocietypublishing.org/doi/10.1098/rspa.2020.0469>.
- [23] Y.-J. Liu, J. Tan, S.-Y. Yu, M. Yousefzadeh, T.-T. Lyu, Z.-W. Jiao, H.-Y. Li, S. Ramakrishna, High-efficiency preparation of polypropylene nanofiber by melt differential centrifugal electrospinning, *J. Appl. Polym. Sci.* 137(3) (2020) 48299, eprint:<https://onlinelibrary.wiley.com/doi/pdf/10.1002/app.48299>. doi: 10.1002/app.48299. URL: <https://onlinelibrary.wiley.com/doi/abs/10.1002/app.48299>.
- [24] R. Thakur, D. Das, A. Das, Optimization study to improve filtration behaviour of electret filter media, *J. The Textile Inst.* 107 (11) (2016) 1456–1462, <https://doi.org/10.1080/00405000.2015.1128207>.
- [25] J. Drabek, M. Zatloukal, Meltblown technology for production of polymeric microfibers/nanofibers: A review, *Phys. Fluids* 31 (9) (2019), 091301, <https://doi.org/10.1063/1.5116336>. URL: <http://aip.scitation.org/doi/10.1063/1.5116336>.
- [26] G. Wypych, PA-3 - polyamide-3 to PZ - polyphosphazene, in: *Handbook of Polymers* (2nd Edition), ChemTec Publishing, 2016, pp. 207–653. URL:<https://app.knovel.com/hotlink/pdf/id:kt010RSOG1/handbook-polymers-2nd/pa-3-polyamide-3>.
- [27] M.P. Bhatnagar, Effect of Rheology and Role of External Forces on Indigenous Melt Centrifugal Spinning of PP fibers and their Transcrystalline Composites (2022) 22 doi:10.26434/chemrxiv-2022-xpv04. URL:<https://chemrxiv.org/engage/chemrxiv/article-details/62e00678a8e4dc7d521d996a>.
- [28] M. Huttunen, M. Kellomäki, A simple and high production rate manufacturing method for submicron polymer fibres, *J. Tissue Eng. Regenerat. Med.* 5 (8) (2011) e239–e243, <https://doi.org/10.1002/term.421>.



Jason Gunther is a Master of Applied Science Student at the Polymer and Composite Engineering Laboratory (LIPEC) group in the Mechanical Engineering Dept. at l'École de Technologie Supérieure (ÉTS), 1100 R. Notre Dame O, Montréal, QC H3C 1K3, Canada. He also graduated at l'ÉTS in Mechanical Engineering. His research subject focuses on producing polymer fibres through the hot melt centrifugal spinning process. He and his team designed a versatile apparatus to share with the scientific community to further understand this process.